

# Shape coexistence and triaxiality in the superheavy nuclei

S. Ćwiok<sup>1\*</sup>, P.-H. Heenen<sup>2</sup> & W. Nazarewicz<sup>3,4,5</sup>

<sup>1</sup>Institute of Physics, Warsaw University of Technology, ul. Koszykowa 75, PL-00662, Warsaw, Poland

<sup>2</sup>Service de Physique Nucléaire Théorique, Université Libre de Bruxelles, CP 229, B-1050 Brussels, Belgium

<sup>3</sup>Department of Physics and Astronomy, The University of Tennessee, Knoxville, Tennessee 37996, USA

<sup>4</sup>Physics Division, Oak Ridge National Laboratory, PO Box 2008, Oak Ridge, Tennessee 37831, USA

<sup>5</sup>Institute of Theoretical Physics, Warsaw University, ul. Hoza 69, PL-00681, Warsaw, Poland

\* Deceased

**Superheavy nuclei represent the limit of nuclear mass and charge; they inhabit the remote corner of the nuclear landscape, whose extent is unknown. The discovery of new elements with atomic numbers  $Z \geq 110$  has brought much excitement to the atomic and nuclear physics communities. The existence of such heavy nuclei hangs on a subtle balance between the attractive nuclear force and the disruptive Coulomb repulsion between protons that favours fission. Here we model the interplay between these forces using self-consistent energy density functional theory; our approach accounts for spontaneous breaking of spherical symmetry through the nuclear Jahn–Teller effect. We predict that the long-lived superheavy elements can exist in a variety of shapes, including spherical, axial and triaxial configurations. In some cases, we anticipate the existence of metastable states and shape isomers that can affect decay properties and hence nuclear half-lives.**

**T**he mere existence of superheavy elements has been a longstanding fundamental scientific problem. How can a nucleus with a large atomic number, such as  $Z = 112$ , survive the huge electrostatic repulsion between the protons? What are its physical and chemical properties?

What is the extent of the superheavy region, that is, is there an upper limit on the number of neutrons and protons that can be bound into one cluster? Do there exist very-long-lived superheavy nuclei?

We know the answers to some of these questions<sup>1</sup>. According to the nuclear shell model, a nucleon—that is, a proton or a neutron—moves in a common potential generated by all the other nucleons. Similar to an electron's motion in an atom, nucleonic orbits bunch together forming shells, and nuclei having filled nucleonic shells (nuclear 'noble gases') are exceptionally stable. This happens for specific 'magic' numbers of protons ( $Z = 2, 8, 20, 28, 50$  and  $82$ ) and neutrons ( $N = 2, 8, 20, 50, 82$  and  $126$ ). The quantum enhancement in nuclear binding due to the presence of nucleonic shells can be quantified in terms of the so-called shell energy<sup>2</sup>. Although the magic nuclei have the largest shell energies, other nuclei can also be shell-stabilized, because the shell energy oscillates strongly with the number of nucleons.

By the end of the 1960s, it had been concluded that the existence of the heaviest nuclei with  $Z > 104$  was primarily determined by the shell effects<sup>3–5</sup>. These early calculations predicted the nucleus with  $Z = 114$ ,  $N = 184$  to be the centre of an island of long-lived superheavy nuclei (see, for example, the discussion in ref. 6). This result stayed practically unchallenged until the late 1990s, when more refined models, based on realistic effective nucleon–nucleon interactions, were applied to superheavy nuclei. The microscopic models are, however, still uncertain when extrapolating in  $Z$  and the mass number  $A$ . In particular, there is no consensus among theorists with regard to what should be the next doubly magic nucleus beyond <sup>208</sup>Pb ( $Z = 82$ ,  $N = 126$ ). In the superheavy nuclei the density of single-particle energy levels is fairly large, so small energy shifts, such as those due, for instance, to poorly known parts of nuclear interaction, can be crucial for determining the shell stability. This situation is similar to that encountered in the chemistry of superheavy elements, where the high density of single-electron states combined with relativistic effects make theoretical predictions

difficult<sup>7</sup>. Modern calculations suggest that the next magic proton shell should appear at higher proton numbers than previously thought:  $Z = 120, 124$  or  $126$ , whereas for the neutrons, most calculations predict magic gaps at  $N = 184$  or  $N = 172$  (refs 6, 8, 9). In contrast to normal nuclei, however, the regions of enhanced shell effects in the superheavy region are generally expected to be fairly broad; that is, the magic gaps are fragile<sup>10</sup>.

At large values of  $Z$  and of the mass number  $A = Z + N$ , the electrostatic repulsion becomes so strong that the nuclear liquid drop becomes unstable to surface distortions<sup>4</sup> and fissions. Because—as discussed below—the quantum shell energy may also favour shape deformation, many superheavy elements seem to be well deformed—that is, the deformed minimum is deep. Indeed, the measured  $\alpha$ -decay energies, along with complementary syntheses of new neutron-rich isotopes of seaborgium ( $Z = 106$ ) and hassium ( $Z = 108$ ), have confirmed the special stability of the deformed nuclei with  $N = 162$  predicted by theory<sup>11–13</sup>.

Beautiful experimental confirmation of large quadrupole shape deformations in the heavy-element region comes from  $\gamma$ -ray spectroscopy around  $Z = 102$ ,  $N = 152$ ; namely, the identification of rotational bands in <sup>254</sup>No and its neighbours (see ref. 14). Figure 1 shows the deformation energies and quadrupole deformations for even–even heavy and superheavy nuclei calculated here. The largest ground-state shape elongations are indeed predicted at around <sup>254</sup>No. The well-deformed elongated (prolate) superheavy nuclei are separated from spherical elements with  $Z = 114–126$ ,  $N = 184$  by the region of weakly deformed, flattened (oblate) nuclei that are candidates for shape isomerism effects or triaxiality<sup>6,15,16</sup>. Here we examined this transitional region, rich in structural phenomena.

## Experimental status

The quest for heavy elements can be divided into several periods<sup>17</sup>. The first period (1896–1940) was characterized by the Curies' work, the first attempts to reach the elements beyond uranium by Fermi and Segre in 1934, and the discovery of nuclear fission in 1938. The Manhattan Project marked the second period (1940–1952), when plutonium became part of the periodic table. The third period (1955–1974) witnessed a Cold War competition between Russian and American laboratories to discover new elements.

The superheavy elements represent the fourth period<sup>13</sup>, which started with the first observations of elements  $Z = 107$ – $109$  at the Gesellschaft für Schwerionenforschung (GSI) in Germany in the beginning of the 1980s. Interest in those exotic species has been rekindled over the last decade, thanks to experimental progress in their synthesis<sup>18–21</sup>. Isotopes of elements with the atomic number  $Z = 110$ – $112$  were discovered at GSI between 1994 and 1996<sup>19</sup>. Those elements are expected to be well-deformed (see Fig. 1) and their lifetimes have been found to be very short. For instance, the isotope  ${}^A Z = {}^{277}112$  turned out to have a half-life of the order of 300  $\mu\text{s}$ . The element 110 (darmstadtium, Ds) was independently confirmed in 2002 by the Lawrence Berkeley Laboratory in the USA<sup>20</sup> and the Institute of Physical and Chemical Research (RIKEN) in Japan<sup>21</sup>. The confirmation of  $Z = 111$  (roentgenium, Rg) and  $Z = 112$  was also made at RIKEN. In a recent experiment, the Japanese physicists have reported the synthesis of  $Z = 113$  ( $A = 278$ )<sup>22</sup>. The production cross-section was found to be rapidly decreasing with the atomic number (it is around 50 pb for  $Z = 113$ ; 1 barn =  $10^{-28}$  m<sup>2</sup>), so it was concluded that it would be very difficult to reach still heavier elements in ‘cold’-fusion reactions using lead or bismuth targets.

The use of ‘hot’-fusion evaporation reactions with the neutron-rich  ${}^{48}\text{Ca}$  beam and actinide targets at the Joint Institute for Nuclear Research in Dubna (Russia) has resulted in measurements of several new elements with  $Z = 113$ – $116$  and 118 (refs 23, 24), including the isotopes of  ${}^{286-290}114$ ,  ${}^{290-293}116$ ,  ${}^{294}118$ , and several new isotopes of  $Z = 110$  and 112. According to Fig. 1, these nuclei, expected to have moderate deformations, belong to the region of shape transition from prolate- to oblate-deformed ground states. The most significant result is the observed increase of half-lives with increasing neutron number. For instance, when going from  ${}^{282}112$  ( $N = 170$ ) to  ${}^{285}112$  ( $N = 173$ ), the half-life increases from 1 ms to 34 s (ref. 25). This is consistent with the predicted increased stability of superheavy elements when approaching  $N = 184$ .

The hot-fusion measurements from Dubna still await confirmation by other laboratories. This is not going to be easy, because these newly synthesized nuclei form an isolated island that is not linked through  $\alpha$ -decay chains with any known nuclei. Therefore, alternative techniques to identify the elements, such as chemistry or very precise mass measurements, are also being pursued.

### Nuclear energy density functional

A theoretical framework aiming at the description of the structure of superheavy nuclei must fulfil several strict requirements. Most importantly, it must be general enough to be confidently applied to a region of the nuclear chart whose properties are largely unknown. Because the universal effective nucleon–nucleon interaction in heavy nuclei has not yet been derived microscopically, the preferred strategy is to use forces adjusted to selected experimental data. This must be done in a way general enough that the resulting effective

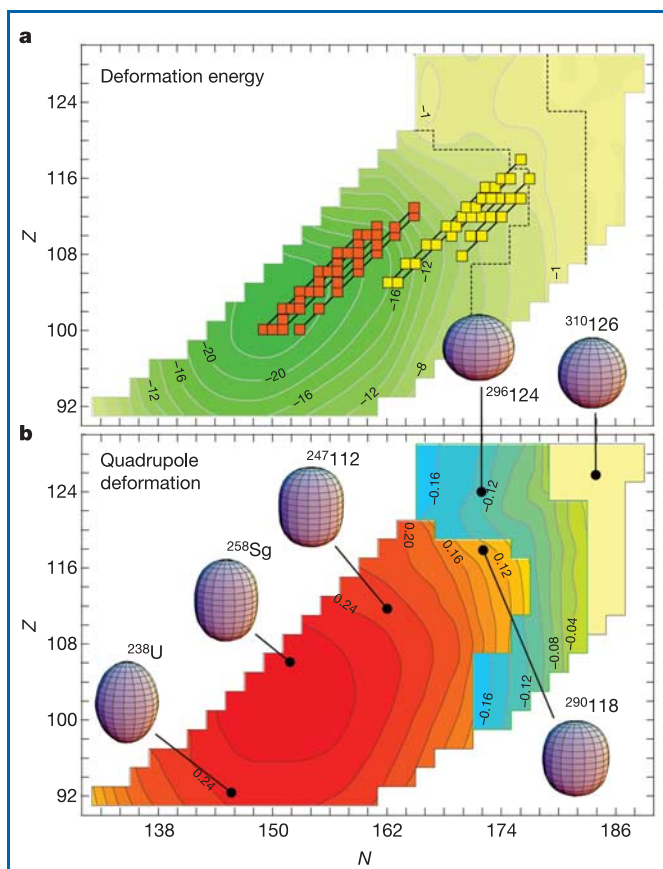


**Figure 1** Deformation properties of even–even superheavy nuclei calculated self-consistently in the  $(N, Z)$ -plane with the SLy4 nuclear energy density functional. The centre of the shell stability is predicted around  $N = 184$ ,  $Z = 126$ . **a**, Deformation energy (in MeV) defined as a difference between the ground-state energy and the energy at the spherical shape. The  $Z = 110$ – $113$   $\alpha$ -decay chains found at GSI and RIKEN are marked by red squares. The  $Z = 118$ , 116, 115 and 114 unconfirmed  $\alpha$ -decay chains reported in Dubna are marked by yellow squares. **b**, Predicted ground-state mass quadrupole deformation  $\beta_2$  (extracted using equation (7) of ref. 6 from the calculated axial mass quadrupole moment  $Q_{20}$ ) and corresponding nuclear shapes for selected nuclei. Prolate shapes ( $\beta_2 > 0$ ) are coloured red–orange, oblate shapes ( $\beta_2 < 0$ ) are blue–green, and spherical shapes ( $\beta_2 = 0$ ) are light yellow.

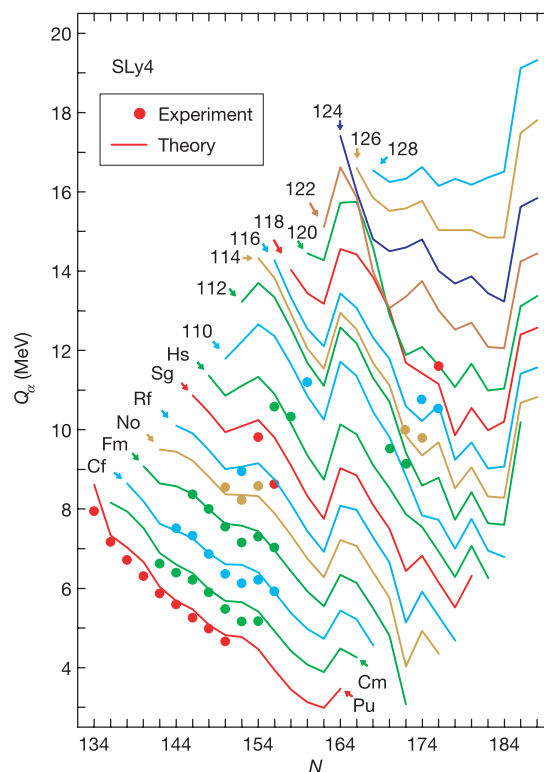


**Figure 2**  $Q_\alpha$  values for even–even nuclei with  $96 \leq Z \leq 118$  obtained in the self-consistent calculations using the energy density functional SLy4. They are compared to experimental data (closed symbols), including the recent Dubna–Livermore data on the  $Z = 116$  and 118  $\alpha$ -decay chains<sup>23,24</sup>. The irregular behaviour of  $Q_\alpha$  as a function of particle numbers can be attributed to shell effects and the resulting deformation changes. (After ref. 1.)

interaction can be used all over the nuclear chart. Another requirement for the method, of particular importance for the superheavy nuclei, is that it must treat correctly the unusually strong interplay between the nuclear and Coulomb forces. Finally, as we show below, studies of superheavy nuclei also require a method that can handle symmetry-breaking effects resulting in a large variety of intrinsic nuclear deformations.

These requirements are met by the density functional theory (DFT) in the formulation of Kohn and Sham<sup>26</sup>. DFT is one of the most popular and successful quantum mechanical approaches to the many-body electronic structure calculations of molecular and condensed matter systems. For many years, it has also been used in many-body nuclear structure calculations<sup>27</sup>. The main ingredient of the nuclear DFT is the energy density that depends on densities and currents representing distributions of nucleonic matter, spins, momentum and kinetic energy, as well as their derivatives (gradient terms). Such density functionals employed in self-consistent mean-field calculations are parameterized by means of about ten coupling constants that are adjusted to basic properties of nuclear matter and to selected data on finite nuclei. They are augmented by the pairing term, which describes nuclear superfluidity<sup>28</sup>. When not corrected by correlation terms, standard nuclear energy functionals reproduce total binding energies with a root-mean-square (r.m.s.) error of the order of 2 to 4 MeV (ref. 29), and they usually perform quite well when applied to energy differences, radii and nuclear moments and deformations<sup>27</sup>.

The self-consistency of the description is guaranteed by applying the Hartree–Fock–Bogoliubov method (HFB). Because all of the nucleons are treated on an equal footing and contribute to single-particle and pairing mean fields, a few hundred nucleonic wavefunctions have to be calculated which makes the computational effort quite demanding. In this work, we consider only ground

states of even–even isotopes. In this case, there is no intrinsic breaking of the time reversal symmetry. We shall use the standard nuclear energy density functional SLy4<sup>30</sup>. Following ref. 6, in the pairing channel, we use the density-independent contact interaction and an approximate particle number projection is carried out by means of the Lipkin–Nogami method. The HFB equations are solved in coordinate space by discretization on a three-dimensional lattice<sup>31</sup>. Figure 2 illustrates the predictive power of our DFT calculations when applied to  $Q_\alpha$  values (that is, energies of the  $\alpha$ -particles emitted by radioactive heavy and superheavy nuclei). Our model reproduces the measured values quite accurately and hence we expect that the SLy4 functional can be reliably applied to as-yet-unobserved superheavy systems.

### Deformed shapes of superheavy nuclei and shape coexistence

The mean-field description of nuclei is performed in a frame of reference attached to the nucleus, the intrinsic frame, in which the nucleus may acquire a deformed shape. The concept of shape deformation is ultimately related to the Jahn–Teller effect (spontaneous symmetry breaking) known in many areas of physics. Symmetry-breaking solutions may appear when, in a mean-field configuration respecting the original symmetries of the nuclear hamiltonian, degenerate single-particle orbits are strongly coupled to collective modes<sup>32</sup>. Figure 1 illustrates the importance of

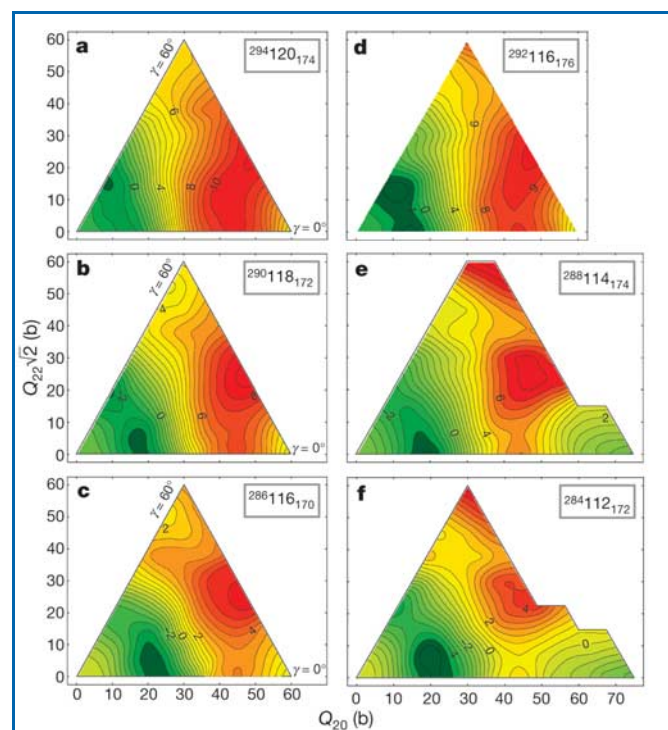


**Figure 3** Potential energy surfaces of the members of the  $\alpha$ -decay chains of  $^{294}_{120}$  (a–c) and  $^{292}_{116}$  (d–f) in the  $(Q_{20}, Q_{22})$  plane calculated with the SLy4 energy density functional. It is seen that both  $\alpha$ -decay sequences are associated with transition from oblate (or triaxial shapes) in the parent nuclei to prolate shapes in lighter daughter nuclei. The difference between contour lines is 0.5 MeV.

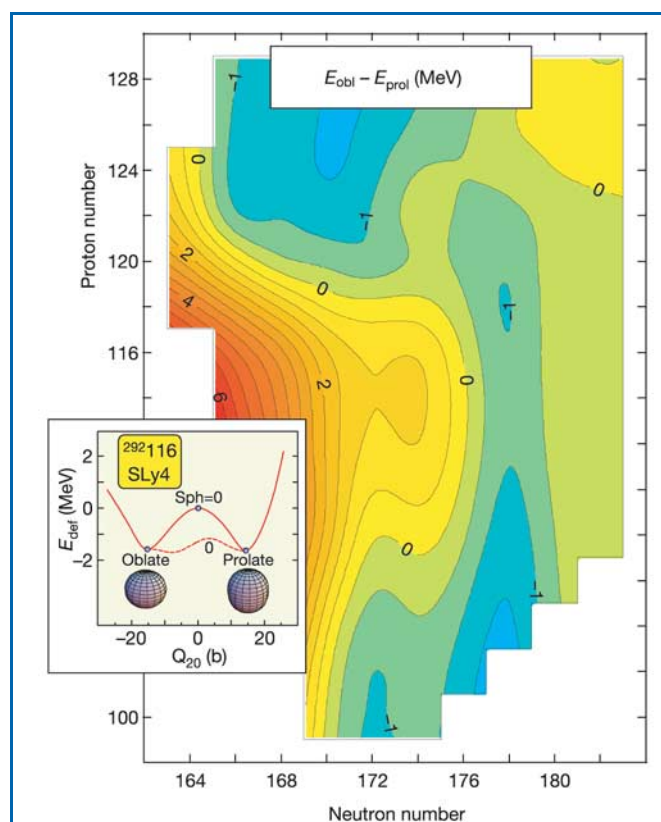


**Figure 4** Contour map of the energy difference between oblate and prolate minima (or saddle points) in the energy surface of superheavy even–even nuclei. Positive (negative) numbers indicate prolate (oblate) ground states. The inset shows the total energy of the superheavy nucleus  $^{292}_{116}$  (recently reported in ref. 23) as a function of the mass quadrupole moment  $Q_0$  along the trajectory of axial shapes ( $\gamma = 0^\circ$ , solid line) and along the trajectory of triaxial shapes ( $\gamma \neq 0^\circ$ , dashed line). We can see that  $^{292}_{116}$  is  $\gamma$ -soft, that is, the inclusion of triaxiality almost completely wipes out the barrier between prolate and oblate minima. However, additional separation between prolate and oblate configurations may exist owing to the presence of intruder orbitals (see text).

the symmetry-breaking effect in the superheavy region. Figure 1a displays the difference between the energies of the spherical and the deformed configurations for the even–even nuclei above uranium. For all the nuclei with at most 118 protons and 172 neutrons, the energy gain due to deformation is larger than 10 MeV. Compared to the total binding energy, the deformation energy seems to be small, but it determines the stability of the nucleus to two main decay modes in this region:  $\alpha$ -emission and spontaneous fission.

Figure 1b shows the variation of the dimensionless mass quadrupole deformation  $\beta_2$  with  $Z$  and  $N$ . All of the isotopes detected at GSI and RIKEN using cold-fusion reactions (marked by red squares in Fig. 1a) are located in a region of large prolate deformations. The heaviest isotopes reported in Dubna’s hot-fusion experiments (yellow squares in Fig. 1a) are predicted to have smaller quadrupole moments and are either oblate or prolate, whereas their decay products lie in a region of rapidly changing shapes. As discussed below, nuclei from this region can be prone to triaxial distortions. (The importance of triaxial shapes in the heaviest and superheavy nuclei, especially in the context of fission, was noted in the early macroscopic–microscopic studies<sup>33–35</sup>.) Only when we approach  $N = 184$  do we expect superheavy nuclei that are spherical in their ground states.

That the shape of a nucleus depends crucially on its proton and neutron numbers is illustrated in Fig. 3, where the variation of the energy as a function of quadrupole moments  $Q_{20}$  and  $Q_{22}$  is plotted for three isotopes belonging to the  $\alpha$  decay chains of <sup>294</sup>120 (Fig. 3a–c) and <sup>292</sup>116 (Fig. 3d–f). The quadrupole moments can be related to the Hill–Wheeler polar deformation parameters  $Q_0$  and  $\gamma$  through the usual relations:  $Q_{20} = Q_0 \cos \gamma$  and  $Q_{22} = \frac{Q_0}{\sqrt{2}} \sin \gamma$ . For weakly deformed shapes,  $Q_0$  is simply proportional to the quadrupole deformation  $\beta_2$ . The deformation parameter  $\gamma$  measures the degree of triaxiality. The  $\gamma = 0^\circ$  limit corresponds to axial prolate shapes ( $\beta_2 > 0$ ) while oblate axial shapes ( $\beta_2 < 0$ ) appear at  $\gamma = 60^\circ$ . Intermediate values of  $\gamma$  are associated with triaxial shapes. The parent nuclei of both  $\alpha$ -chains have near-oblate ground states; their daughters are calculated to be prolate, but with a very small barrier with respect to triaxial deformation  $\gamma$ . The ground states of the

lightest isotopes shown in Fig. 3 are expected to have near-prolate deformations.

To illustrate the prolate–oblate energy balance in the superheavy nuclei, Fig. 4 displays the energy difference between the oblate and prolate minima (which are sometimes only saddle points in the  $\gamma$  direction). The prolate ground states usually correspond to minima that are fairly deep; however, for the oblate ground states, the prolate configurations are, in most cases, excited by less than 1 MeV. Experimentally, one can thus expect the coexistence of  $J^\pi = 0^+$  states close in energy that result from the mixing of configurations having different shapes. This phenomenon, called shape coexistence<sup>36</sup>, is known in nuclei from several regions of the nuclear chart.

The single-neutron and single-proton energy levels plotted in Fig. 5 explain the origin of the shape change along the  $\alpha$ -decay chains shown in Fig. 3 and the oblate–prolate competition of Fig. 4. The single-particle levels have been calculated for the nucleus <sup>292</sup>116, but they are very similar for the six nuclei in question. The large gaps in the single-particle spectrum can be associated with increased stability of a given nuclear shape. For instance, the increased shell stability at particle numbers  $N = 184$  and  $Z = 126$  can be attributed to the corresponding spherical gaps in the single-particle spectrum. These gaps of about 2–3 MeV are, however, much smaller than the magic gaps in the known doubly magic nuclei<sup>9,10</sup>. Therefore, deformation effects can play a particularly important role in the superheavy systems. It is the interplay between the pronounced oblate gaps at  $Z = 120$  and  $N = 172, 178$ , and the large prolate gaps at  $Z = 114, 116$  and  $N = 174, 176$  that determines the microscopical shape coexistence and shape-transitional behaviour in this region.

Figure 5b and d display the single-particle energies as a function of  $\gamma$  for  $Q_0 = 15$  b, which corresponds to the path connecting the prolate and the oblate minima. For  $N \approx 176$  and  $Z \approx 120$ , the density of states around the Fermi level is very low in the  $\gamma$  direction, which explains the large softness of the calculated binding energy against  $\gamma$  (see inset in Fig. 4). Therefore, we expect that dynamical correlation effects associated with the large-amplitude collective motion in the  $\gamma$  direction will be large for most transitional nuclei

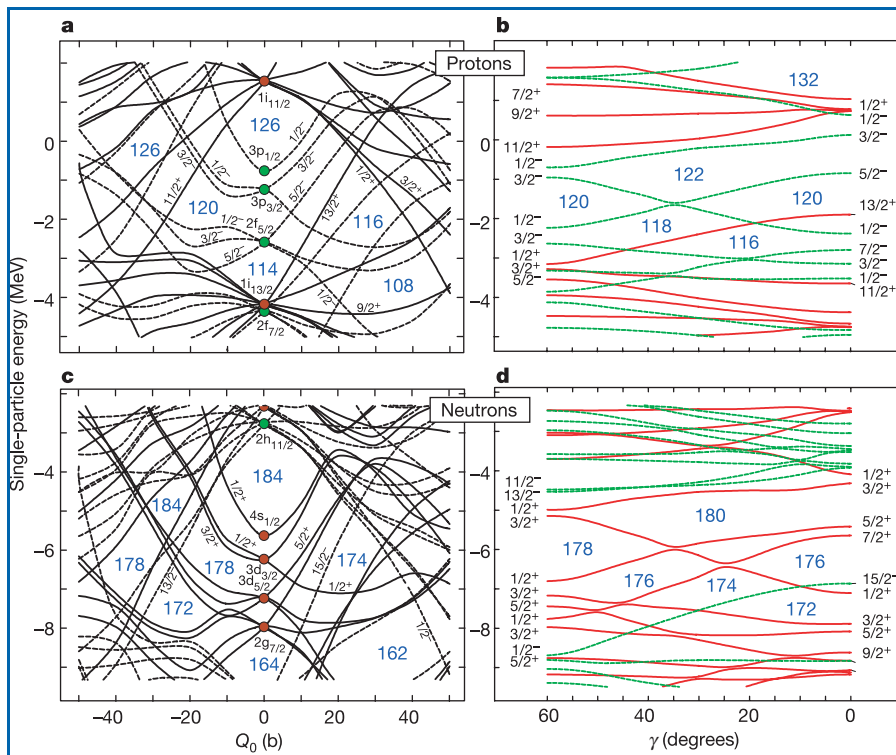


**Figure 5** Single-proton (a, b) and single-neutron (c, d) energy levels in the superheavy nucleus <sup>292</sup>116<sub>176</sub> obtained in self-consistent calculations with the SLy4 energy density functional. Solid and dashed lines mark positive-parity and negative-parity levels, respectively. a, c, Single-particle energies as a function of the mass quadrupole moment  $Q_0$  ( $\gamma = 0^\circ$ ). Positive (negative) values of  $Q_0$  correspond to prolate (oblate) shapes. At the spherical point, nucleonic shells are labelled using the spherical quantum numbers ( $n_j$ ), whereas the deformed orbitals are labelled using two quantum numbers  $\Omega^\pi$ , where  $\Omega$  is the projection of the single-particle angular momentum on the symmetry axis and  $\pi$  is parity. b, d, The dependence of single-particle energies on triaxial deformation  $\gamma$  at a fixed value of  $Q_0 = 15$  b. The  $\Omega^\pi$  labels are shown only at  $\gamma = 0^\circ$  (axial prolate shape) and  $\gamma = 60^\circ$  (axial oblate shape). The large spherical and deformed subshell closures are indicated.

considered; they will lead to the spreading of the nuclear wavefunction in the direction of  $\gamma$ .

It has to be noted, however, that the softness of the total energy surface is not the whole story. There are numerous situations in which some specific single-particle structure can give rise to a strong separation between coexisting minima in the many-body configuration space, even if the potential barrier between the minima is very small or even nonexistent. Usually, the separation can be associated with an occupation of specific single-particle orbitals with very distinct quantum characteristics, the so-called ‘intruder states’<sup>36</sup>. In Fig. 5, we notice the presence of two such intruder levels, which at  $\gamma = 0^\circ$  carry a very large projection of the single-particle angular momentum  $\Omega$  on the symmetry axis. Those are the  $\Omega^\pi = 13/2^+$  proton level (appearing just below the prolate gap at  $Z = 120$ ) and the  $\Omega^\pi = 15/2^-$  neutron level (appearing just below the prolate gap at  $N = 176$ ). Both levels originate from the high- $j$  unique parity spherical shells  $\pi i_{13/2}$  and  $\nu j_{15/2}$ , respectively. For proton numbers  $Z = 116$  and  $118$ , the  $\Omega^\pi = 13/2^+$  proton level is clearly occupied at an oblate shape, and empty at a prolate shape. Likewise, at  $N = 168$ – $172$  the  $\Omega^\pi = 15/2^-$  neutron is occupied (empty) at an oblate (prolate) configuration. In nuclei with those particle numbers, we expect coexistence between prolate and oblate shapes and that quantum correlations will not destroy the simple mean-field picture of shape coexistence. In other cases, our calculations suggest  $\gamma$ -softness and strong configuration mixing.

## Discussion

The new theoretical results presented in this work were obtained in the self-consistent formalism based on a modern nuclear energy density functional. We performed calculations for the even–even heavy and superheavy nuclei with  $Z \leq 128$  and  $N \leq 188$ . Our main conclusions can be summarized as follows:

- (1) The large electrostatic repulsion and large single-particle level density around the Fermi level mean that deformation effects play a particularly important role in the description of superheavy elements. Although the actinide and transfermium nuclei are known to possess well-deformed elongated shapes, the superheavy elements around  $Z = 116$  and  $N = 176$  are expected to exhibit coexistence of oblate and prolate shapes.
- (2) The inclusion of triaxiality can dramatically reduce the barrier separating prolate and oblate minima, leading to structures that are soft or unstable to triaxial distortions.
- (3) In most cases, the underlying single-particle configurations change gradually (adiabatically) along the triaxial energy surface. Hence, strong anharmonicities and large dynamical effects are likely. In some cases, however, (diabatic) prolate and oblate states are expected to be well separated in the configuration space, thanks to the presence of high- $\Omega$  intruder levels originating from high- $j$  shells.
- (4) The heaviest isotopes recently reported in Dubna are predicted to belong to a transitional region strongly influenced by dramatic shape changes and/or triaxial softness. Such shape effects are expected to affect  $\alpha$ -decay lifetimes in two ways. First, the deformation affects the energy of  $\alpha$ -decay,  $Q_\alpha$ . Second, we expect transitions involving parent and daughter nuclei with different shapes to be hindered. This may explain the observation of longer half-lives for some nuclei within these decay chains. Consequently, the existence of shape isomers in the superheavy nuclei may make the identification of the new species more difficult.  $\square$

doi:10.1038/nature03336.

1. Heenen, P.-H. & Nazarewicz, W. Quest for superheavy nuclei. *Europhys. News* **33**, 1–9 (2002).

2. Strutinsky, V. M. Shells in deformed nuclei. *Nucl. Phys. A* **122**, 1–33 (1967).
3. Sobczewski, A., Gareev, F. A. & Kalinkin, B. N. Closed shells for  $Z > 82$  and  $N > 126$  in a diffuse potential well. *Phys. Lett.* **22**, 500–502 (1966).
4. Myers, W. D. & Swiatecki, W. J. Nuclear masses and deformations. *Nucl. Phys.* **81**, 1–60 (1966).
5. Nilsson, S. G. *et al.* On the nuclear structure and stability of heavy and superheavy elements. *Nucl. Phys. A* **131**, 1–66 (1969).
6. Ćwiok, S., Dobaczewski, J., Heenen, P.-H., Magierski, P. & Nazarewicz, W. Shell structure of the superheavy elements. *Nucl. Phys. A* **611**, 211–246 (1996).
7. Schwerdtfeger, P. & Seth, M. B. in *Encyclopedia of Computational Chemistry* Vol. 4, 2480–2494 (Wiley, New York, 1998).
8. Bender, M., Rutz, K., Reinhard, P.-G., Maruhn, J. A. & Greiner, W. Shell structure of superheavy nuclei in self-consistent mean-field models. *Phys. Rev. C* **60**, 034304 (1999).
9. Kruppa, A. T. *et al.* Shell corrections of superheavy nuclei in self-consistent calculations. *Phys. Rev. C* **61**, 034313 (2000).
10. Bender, M., Nazarewicz, W. & Reinhard, P.-G. Shell stabilization of super- and hyperheavy nuclei without magic gaps. *Phys. Lett. B* **515**, 42–48 (2001).
11. Ćwiok, S., Pashkevich, V. V., Dudek, J. & Nazarewicz, W. Fission barriers of transfermium elements. *Nucl. Phys. A* **410**, 254–270 (1983).
12. Möller, P. & Nix, J. R. Stability of heavy and superheavy elements. *J. Phys. G* **20**, 1681–1747 (1994).
13. Armbruster, P. On the production of superheavy elements. *Acta Phys. Polon. B* **34**, 1825–1866 (2003).
14. Julin, R. In-beam spectroscopy of heavy actinides. *Nucl. Phys. A* **685**, 221–232 (2001).
15. Ren, Z. Shape coexistence in even-even superheavy nuclei. *Phys. Rev. C* **65**, 051304 (2002).
16. Bürvenich, T., Bender, M., Maruhn, J. A. & Reinhard, P.-G. Systematics of fission barriers in superheavy elements. *Phys. Rev. C* **69**, 014307 (2004).
17. Hoffman, D. C., Ghiorso, A. & Seaborg, G. T. *The Transuranium People* (World Scientific, River Edge, New Jersey, 2000).
18. Hofmann, S. & Münzenberg, G. The discovery of the heaviest elements. *Rev. Mod. Phys.* **72**, 733–767 (2000).
19. Hofmann, S. *et al.* Properties of heavy nuclei measured at the GSI SHIP. *Nucl. Phys. A* **734**, 93–100 (2004).
20. Ginter, T. N. *et al.* Confirmation of production of element 110 by the  $^{208}\text{Pb}(^{64}\text{Ni},n)$  reaction. *Phys. Rev. C* **67**, 064609 (2003); erratum **C68**, 029901 (2003).
21. Morita, K. *et al.* Status of heavy element research using GARIS at RIKEN. *Nucl. Phys. A* **734**, 101–108 (2004).
22. Morita, K. *et al.* Experiment on the synthesis of element 113 in the reaction  $^{209}\text{Bi}(^{70}\text{Zn},n)^{278}113$ . *J. Phys. Soc. Jpn.* **73**, 2593–2596 (2004).
23. Oganessian, Yu. Ts. *et al.* Heavy element research at Dubna. *Nucl. Phys.* **734**, 109–123 (2004).
24. Moody, K. & the Dubna–Livermore Collaboration. Superheavy element isotopes, decay properties. *Nucl. Phys. A* **734**, 188–191 (2004).
25. Oganessian, Yu. Ts. *et al.* Measurements of cross sections for the fusion-evaporation reactions  $^{244}\text{Pu}(^{48}\text{Ca},xn)^{292-x}114$  and  $^{245}\text{Cm}(^{48}\text{Ca},xn)^{293-x}116$ . *Phys. Rev. C* **69**, 054607 (2004).
26. Kohn, W. & Sham, L. J. Self-consistent equations including exchange and correlation effects. *Phys. Rev. A* **140**, 1133–1138 (1965).
27. Bender, M., Heenen, P.-H. & Reinhard, P.-G. Self-consistent mean-field models for nuclear structure. *Rev. Mod. Phys.* **75**, 121–180 (2003).
28. Perlińska, E., Rohozinski, S. G., Dobaczewski, J. & Nazarewicz, W. Local density approximation for proton-neutron pairing correlations: formalism. *Phys. Rev. C* **69**, 014316 (2004).
29. Stoitsov, M. V., Dobaczewski, J., Nazarewicz, W., Pittel, S. & Dean, D. J. Systematic study of deformed nuclei at the drip lines and beyond. *Phys. Rev. C* **68**, 054312 (2003).
30. Chabanat, E., Bonche, P., Haensel, P., Meyer, J. & Schaeffer, R. A Skyrme parametrization from subnuclear to neutron star densities. Part II: nuclei far from stabilities. *Nucl. Phys. A* **635**, 231–256 (1998).
31. Bonche, P., Flocard, H., Heenen, P.-H., Krieger, S. J. & Weiss, M. S. Self-consistent calculation of triaxial deformations: application to the isotopes of Kr, Sr, Zr, and Mo. *Nucl. Phys. A* **443**, 39–63 (1985).
32. Nazarewicz, W. Microscopic origin of nuclear deformations. *Nucl. Phys. A* **574**, 27c–49c (1994).
33. Pashkevich, V. V. The energy of non-axial deformation in heavy nuclei. *Nucl. Phys. A* **133**, 400–404 (1969).
34. Larsson, S. E., Ragnarsson, I. & Nilsson, S. G. Fission barriers and the inclusion of axial asymmetry. *Phys. Lett. B* **38**, 269–273 (1972).
35. Götz, U., Pauli, H. C. & Junker, K. Influence of asymmetric distortions on fission barriers. *Phys. Lett. B* **39**, 436–438 (1972).
36. Wood, J. L., Heyde, K., Nazarewicz, W., Huysse, M. & Van Duppen, P. Coexistence in even-mass nuclei. *Phys. Rep. C* **215**, 101–201 (1992).

**Acknowledgements** We thank M. Bender, J. Dobaczewski and M. Stoyer for discussions. This work was supported in part by the US Department of Energy, by the National Nuclear Security Administration under the Stewardship Science Academic Alliances programme, by the Belgian Science Policy Office, by NATO, and by the Polish Committee for Scientific Research (KBN).

**Competing interests statement** The authors declare that they have no competing financial interests.

**Correspondence** and requests for materials should be addressed to P.-H.H. (phheenen@ulb.ac.be).